Monitoring Snowmelt in the Canadian High Arctic Using a DEM and Remote Sensing

DAVID R.M. JONES[1] AND KATHY L. YOUNG

ABSTRACT

Previous snow accumulation studies on Cornwallis Island have been conducted at a 16 x 13 km target site. A simple landscape classification of the site was used as a basis for snow cover measurement. This study aims to improve the initial landscape classification process via analysis of a DEM, and validate predicted snowmelt based on a simplified energy balance model, using remotely sensed data. In conclusion it is argued that a more accurate and complete landscape classification was achieved, but validation reveals discrepancies between modelled and actual snowmelt.

Keywords: High Arctic, snowmelt, landscape classification, validation.

INTRODUCTION

Large scale modeling of arctic snow distribution, in particular with regard to the timing and duration of the critical snowmelt period, has become increasingly important in the context of monitoring and predicting global environmental change. During snowmelt significant changes occur in the surface energy balance, mainly as a function of the reduction in albedo as snowcover gives way to bare ground. Also of great importance is the associated peak in surface water run-off, and the implications for hydrology (e.g. soil moisture).

Previous studies of snow cover at an intermediate grid scale (1 km) have been conducted on Cornwallis Island, for a 16 x 13 km site in the island's interior (Woo *et al*., 1999). Snowcover for this target site was calculated using two major steps. Firstly, a landscape classification was produced based on an interpretation of a topographic map and aerial photos. This classification was used to conduct terrain-based snow surveys of various terrain units, yielding mean values of snow water equivalent (SWE) for each terrain class, and averaged for each 1 km grid.

The main goal of this study is to improve upon this sequence of events. There are two major objectives. The first objective is to improve the landscape classification process through the analysis of a digital elevation model (DEM), thereby improving snowcover information. By using automated techniques for the classification, it was hoped to remove operator bias. Secondly, validation of the snowmelt model outputs by using Landsat-7 satellite imagery is conducted. This paper presents the preliminary results of the study, detailing the process of landscape classification, outlining the snowmelt modelling procedure, and comparing predicted snow cover with actual snowcover, as derived by two Landsat-7 images of the study area during snowmelt.

---

[1] Department of Geography, York University, 4700 Keele Street, Toronto, Ontario. M3J 1P3; Telephone: 416-736-5107 Fax: 416-736-5988 E-mail: drmjones@yorku.ca, klyoung@yorku.ca

STUDY AREA

Field research was conducted during the 2000 spring snowmelt season on Cornwallis Island, Nunavut. Field work was based from the Polar Continental Shelf Project (PCSP) base (74˚43'07" N, 94˚59'19" W) near Resolute, on the south-west coast (Figure 1). Cornwallis Island is characterized as a polar desert environment, with a mean annual precipitation of 138 mm and mean maximum monthly temperature in July of 4.2°C. Vegetation is sparse, covering no more than 20 % of the total land area (Edlund, 1992).
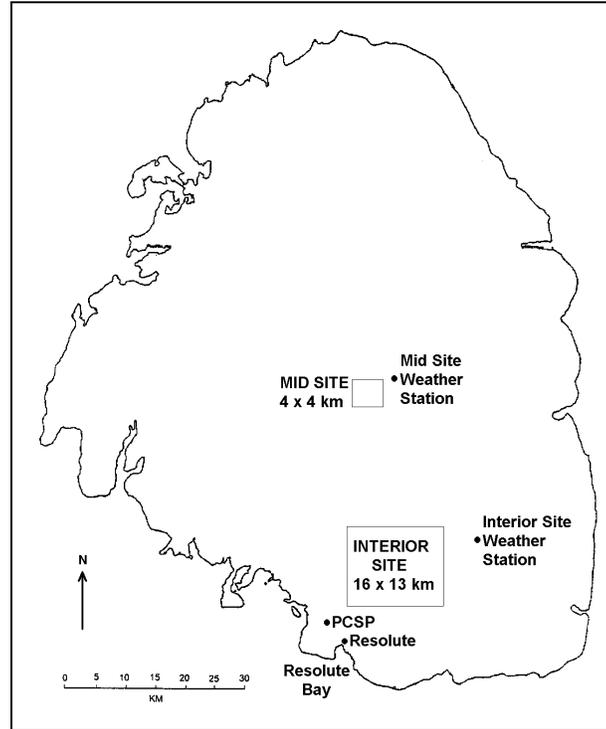

Figure 1. Study area and study sites.

Two main study sites were selected for the investigation of snowcover and melt (Figure 1). The first of these, the Interior Site, matches that studied by Woo *et al.* (1999), and is 16 x 13 km in extent (208 km^2) to the north-east of PCSP (bottom left 74˚45'11 N", 94˚56'32" W; top right 74˚52'25" N, 94˚24'28" W). The landscape in this site is predominately non-vegetated, with large areas of relatively flat land and several major drainage basin systems, which gives rise to extensive dissected topography in the upper sector of the site. A second site was also investigated, a Mid Site (bottom left 75˚06'10" N, 94˚57'06" W; top right 75˚08'23" N, 94˚49'00" W), which for logistical reasons was much smaller, at 4 x 4 km in extent (16 km^2), than the Interior site. The Mid Site is located near the geographic center of the island.

Adjacent to each of these target sites were placed meteorological towers with the necessary instrumentation to record hourly information relating to the surface energy balance. Both stations recorded air temperature, relative humidity, wind speed and wind direction, net radiation, incoming and outgoing shortwave radiation and rainfall, at one minute intervals averaged over the hour. Also available at the Mid Site station was a thermocouple nest measuring vertical snow temperature at 50 mm intervals within the snowpack.

The permanent Environment Canada weather station at Resolute Airport (74° 43' N, 94° 59' W) additionally collected barometric pressure, utilized in the snowmelt calculation.

METHODS

Terrain Classification.

The terrain classification system was designed with several factors in mind. A balance had to be reached between adequately representing landscape variability while keeping the subsequent field work logistically possible, in terms of acquiring adequate snow cover information for each class. The classes selected (cf. Mitchell, 1991) were primarily based on gradient and aspect. They were 'flat' areas (<2°), subdivided into Plateau (≥150 m) and Lowland (<150 m), slopes of various aspect (≥2°<40°) composed of N, NE, E, SE, S, SW, W & NW aspects, and Lakes. Only one gradient category was chosen because with two classes (2-19º, 20-40º), only very small areas were defined as 20-40º in the GIS classification. Also, it was unsafe to sample steeper slopes in the field. A 1:250,000 scale DEM was analyzed to extract these landscape types. Resultant images were interpreted to produce a composite terrain unit map (Figure 2). Comparison with a 1:50,000 topographic map, however, revealed inconsistencies in the classification process, hence the DEM-derived classification was modified to conform more tightly to the topographic map (Figure 3). The errors seen in the DEM classification are due to the small scale of the DEM itself. The level of detail needed to create an accurate portrayal of the landscape simply is not available. In total, 98 individual terrain units make up the Interior Site, which differs from the 23 of Woo *et al*. (1999).
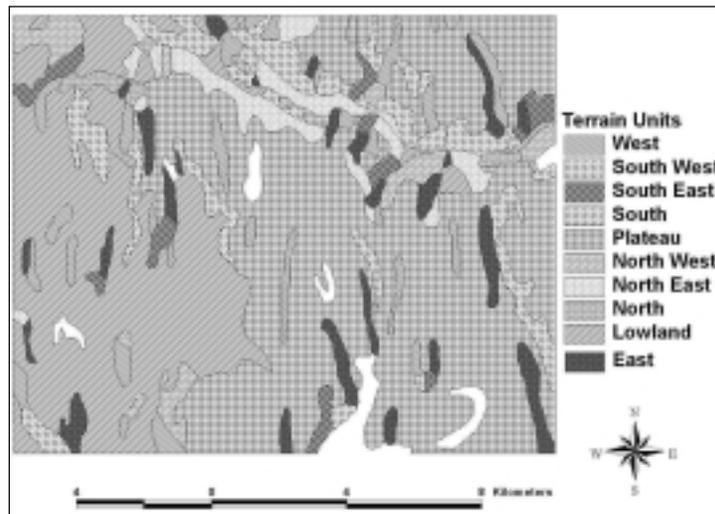

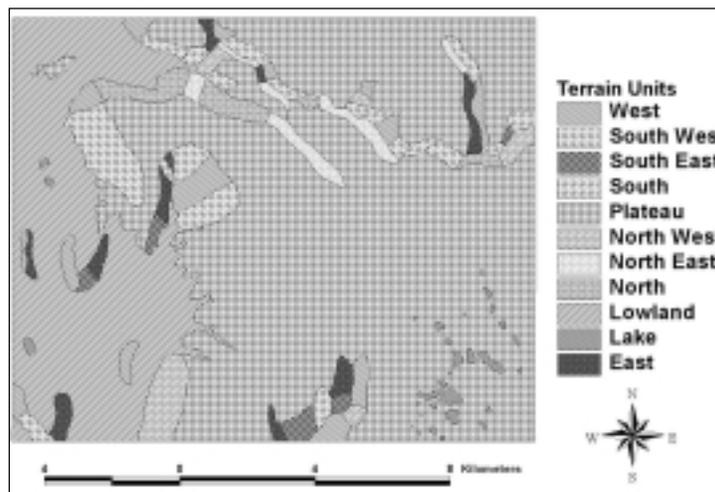Figure 2. DEM-derived landscape classification map.

Figure 3: Revised landscape classification map.

Snow Cover Estimation.

Using the terrain classified maps for each site, transect lines (0.15 to 6.0 km in length) were selected to pass through each terrain type several times in order to achieve a robust average snow cover value (see Figure 4, below). Field sampling procedure followed that described by Woo (1997). Along each transect line snow depth was measured at regular intervals (5 to 20 points, depending on transect length), with an average of four depths at each point taken to reduce variabilty. Snow density was measured an average of three times per transect, since variation in snow density is minimal over space (Woo *et al.*, 1983). Mean depth and density values for each class were calculated, and SWE derived. Grid values for all three variables (snow depth, density and water equivalent) were acquired by weighting each grid by terrain class percentage. The Interior Site was sampled on Julian Days 158-159 (June 6/7) and the Mid Site on Julian Day 161 (June 9).

Figure 4. Transect lines used at the Interior Site (16 x 13 km).
Solid lines = sampled, dashed lines = traversed terrain.

Snowmelt Calculation.

Point meteorological information acquired for each site was used as an input to a physically-based snowmelt model, described by:

$$Q_M = Q^* + Q_H + Q_E + Q_P \qquad\qquad (1)$$

where Q_M is energy available for melt, Q^* is net radiation, Q_H is sensible heat flux, Q_E is latent heat flux, and Q_P melt energy delivered by precipitation (rain). Q^* was measured directly by a net radiometer, while Q_H and Q_E were calculated using the bulk energy transfer approach (see Price & Dunne, 1976). Variables therefore included air temperature, relative humidity, and wind speed. Snow surface temperature (derived from air temperature of the present and past hour, as described by Marsh & Pomeroy, 1996) was also included in the model. Q_M is converted into snowmelt by:

$$M = Q_M/(\lambda\rho), \text{ if } Q_M > 0 \qquad\qquad (2)$$
$$= 0, \text{ otherwise}$$

where λ is the latent heat of fusion, and ρ is the density of water. The base station data were transferred to each terrain unit on the basis of elevation and aspect. A lapse rate of 0.01°C/m (established by Woo *et al.*, 1999) was used to modify air temperature with elevation. Air pressure from the Resolute weather station was modified by elevation according to Brutsaert's (1975) equation. Wind speed was modified for slopes using empirical relationships established by Woo &

Young (2000). A deficiency of the present model is that no correction was made for Q* from the base station. The reason being that a large part of the target area (82 %) is relatively flat and verification of the model response would generally be directed to these areas

Snowmelt was therefore calculated for each terrain unit, on a daily basis. Grid equivalents of melt were determined by weighting each grid cell by percentage terrain unit. Daily snowmelt maps from the time of snow survey until the complete ablation of snow cover were therefore produced (Figures 8 & 9).

Validation.

Two Landsat-7 scenes were acquired over the study area, for Julian Days 168 and 173 (June 16 and 21). After calibration and geo-referencing was completed, the study site areas were extracted from the panchromatic band (channel 8) and classified into two classes using a supervised minimum distance classification procedure (Figures 10 & 11) (cf. Richards & Jia, 1999).

The accuracy of the snow cover classification appears to be quite good. Training sites for each land cover type (snow/snow-free) at each site were carefully selected, and this supervised technique is a vast improvement over unsupervised approaches. Comparison with the respective pan images show accurate classification on both days.

RESULTS & DISCUSSION

Snow depth data is compared between each site in Figure 5, and among terrain classes for the Interior Site in Figure 6.
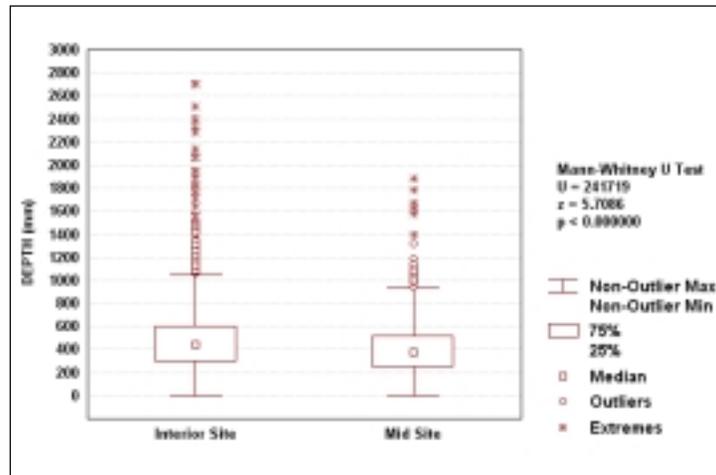

Figure 5. Snow depth at the Interior and Mid Site.

Mean snow depth measured at the Interior and Mid Sites is 509 and 411 mm, respectively, with a much larger range at the Interior Site (0-2704 mm) than the Mid Site (0-1882 mm). Standard deviations are 359 and 266 mm, respectively. Visually, snow depth does not appear to vary substantially between the two sites, yet statistically there is a significant difference. A Mann-Whitney U Test (a non-parametric test of variance) determined a significant p-value (<0) between snow depth at the Interior Site and Mid Site (Figure 5). This can be partially explained by the fact that snow data collection at each site was two to three days apart, and some melt was evident during that time (2.7 mm SWE, at the Interior met station). Also, there is considerably more data for the Interior Site (1214 snow depth values) than the Mid Site (484 snow depth values), and there are many more outliers and extremes for the Interior site, due to the more extreme topography here.

For between-unit variation, Figure 9 shows the Interior Site data. The flat areas (Plateau, Lowland) have quite similar snow depths (556 and 447 mm, respectively), whereas there is a wide

range of depths between the slope aspects (from 401 mm for South East to 879 for West). These results demonstrate the effects of wind re-distribution on snow cover (e.g. Donald *et al*., 1995).
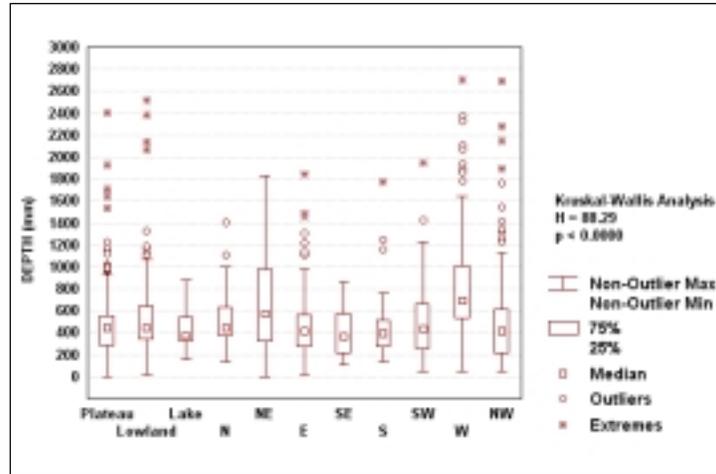

Figure 6. Snow depth by terrain class, Interior Site.

Snowmelt energy fluxes can be seen in Figure 7. The dominant flux contributing to melt is radiation, followed by sensible heat flux. This is common for high arctic environments and has been observed by others (e.g. Woo *et al*., 1999; Young & Lewkowicz, 1990). The main melt period can be considered to commence from about Julian Day 162, with a sustained positive energy flux density occurring.
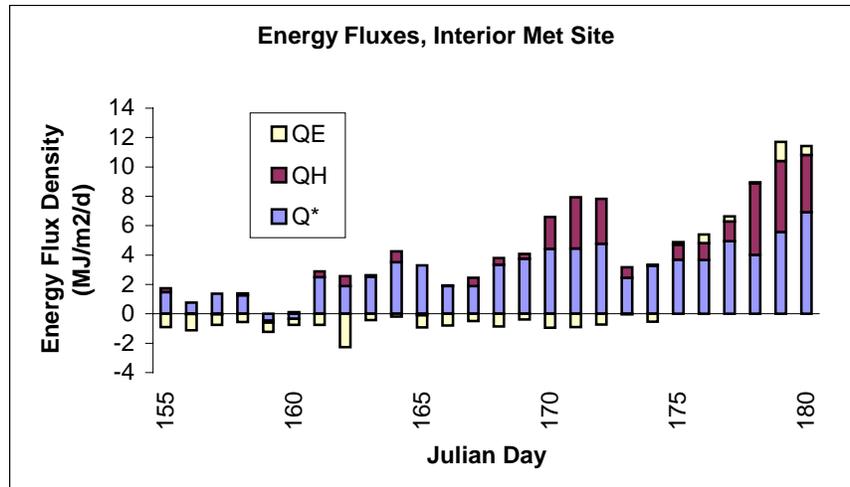

Figure 7. Energy fluxes at the Interior Site meteorological station, Julian Day 155 to 180 (June 3 to June 28).

Snowmelt maps tracking the gradual ablation of snow cover through time were produced. The maps show smoothed grid SWE information for the Interior site. Data for Julian Days 168 (6 days after main melt began) and 173 (11 days after main melt) are shown here (Figures 8 & 9). The main features of both these maps are the high peaks in remaining SWE at specific locations, coinciding with the aforementioned West and North-East facing slopes, which had higher than average snow depths. On both days, the Lowland and Plateau flat areas can be distinguished by the major contour line on the left-hand side of each map. By Julian Day 173, the model predicts

that the majority of the snow in the interior site has ablated (38 % remains). The whole site is predicted to have completely melted by Julian Day 178. At the Mid Site (not shown), snow cover is predicted to have completely disappeared on Julian Day 177, one day sooner than the Interior Site.
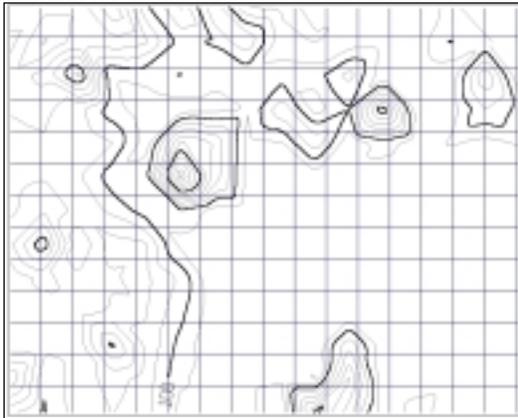

Figure 8. Predicted SWE values (60-190mm), Julian Day 168. Contour interval = 10 mm.
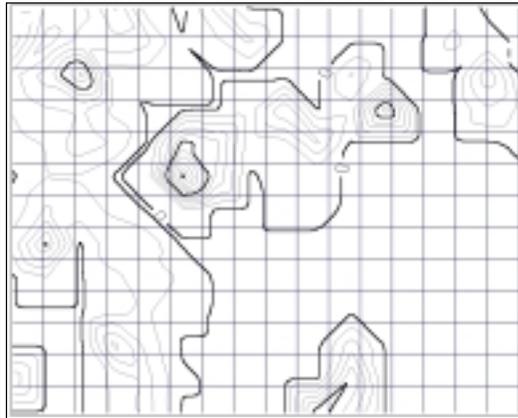
Figure 9. Predicted SWE values (0-100mm), Julian Day 173. Contour interval = 10 mm.

The corresponding classified Landsat-7 panchromatic scenes for the Interior Site on Julian Day 168 and Julian Day 173 (Figures 10 & 11) show some differences to predicted snow cover. The Julian Day 168 snowmelt map suggests 100 % snow coverage, the classified Landsat image shows snow cover of 91 %. This is early on in melt so the discrepancy is small. But by Julian Day 173, predicted melt suggests only 39 % of snow remains, and the corresponding Landsat scene is 72 %. Clearly, this second date reveals a significant discrepancy in predicted versus actual melt. Whereas the model predicts a mostly snow-free plateau area, the Landsat image shows virtually the opposite, with the Lowland areas mostly snow-free.

Some of the differences can be explained by the difference in resolution of the respective results. Predicted values are at a 1 km grid resolution; the Landsat panchromatic band offers 15 m spatial resolution. Such large differences in scale are not easy to reconcile (Bloschl, 1999). At the Mid Site, the differences between predicted and actual melt are much smaller than at the Interior Site, which is encouraging. On Julian Day 168 predicted snow cover is 100 % and classified is 89 %. On Julian Day 173, the figures are very similar, at 73 and 72 %, respectively (flat area comprises 65 %).
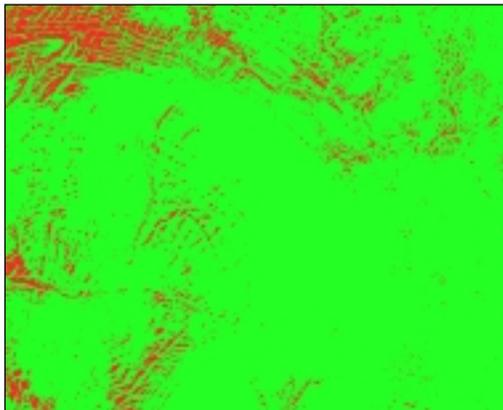

Figure 10. Classified Landsat-7 pan scene, Julian Day 168, Interior Site. Lighter tone is snow cover, darker tone snow free.
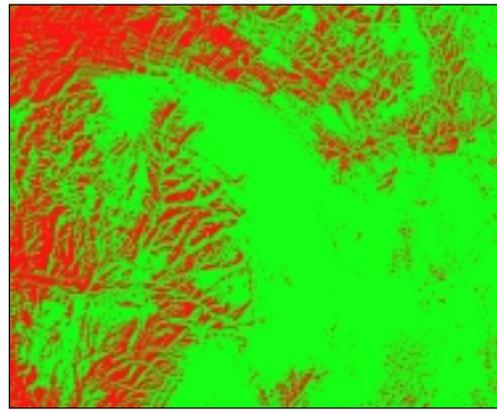
Figure 11. Classified Landsat-7 pan scene, Julian Day 173, Interior Site. Lighter tone is snow cover, darker tone snow free.

Unfortunately, no optical imagery is available around Julian Days 177/178 (when each site is predicted to become completely snow free) due to cloud cover over the study areas. This would be very useful since it would provide a more conclusive verification of predicted melt for the Interior

Site. Predicted snowmelt should improve when the model allows for the distribution of radiation over varying terrain types.

CONCLUSIONS

The first major objective, to improve the landscape classification of the main Interior Site, was to a certain extent a success. A more accurate and detailed classification of the target area was achieved, however this was not achieved quantitatively, as was first envisaged. The resolution of the DEM (1:250,000) used to extract terrain information was inadequate, when compared to the larger scale topographic map (1:50,000).

Predicted snowmelt, when compared with the classified remotely sensed images on two separate dates, gives mixed results. At the Interior Site, there is large discrepancy between predicted and actual melt on Julian Day 173 (June 21). However, modelled melt at the Mid Site appears to have been more successful. Caution is needed, however, because of the differences in scale of predicted and actual melt patterns, and also the fact that only two dates are available for comparison.

REFERENCES

Blöschl, G. (1999) 'Scaling issues in snow hydrology,' *Hydrological Processes*, **13**, (14/15) 2149-2175.

Brutseart, W. (1975) 'On a derivable formula for long-wave radiation from clear skies,' *Water Resources Research*, **11**, 742-744.

Donald, J.R., Soulis, E.D., Kouwen, N. & Pietroniro, A. (1995) 'A land cover-based snow cover representation for distributed hydrological models,' *Water Resources Research*, **31**, 995-1009.

Edlund, S.A. (1992) 'Vegetation of Cornwallis and adjacent islands, Northwest Territories: Relationships between vegetation and surficial materials,' *Geological Survey of Canada*. Paper 89-26. 24 pp.

Mitchell, C. (1991) *Terrain Evaluation*. Longman Scientific and Technical, London, UK. 441 pp.

Richards, J.A. & Jia, X. (1999) *Remote sensing digital image analysis: an introduction*. (3rd ed). 363 pp.

Price, A.G. & Dunne, T. (1976) 'Energy balance computations of snowmelt in subarctic area,' *Water Resources Research*, **12**, 686-694.

Woo, M.k. (1997) 'A guide for ground based measurement of the Arctic snow cover,' Report for Atmospheric Environment Service. Submitted Draft.

Woo, M-k., Marsh, P. and Steer, P. (1983) 'Basin water balance in a continuous permafrost environment,' *Proceedings Fourth International Conference on Pemafrost, Fairbanks, Alaska*, 1407-1411.

Woo, M-k., Yang, D. & Young, K.L (1999) 'Representation of arctic weather station data for the computation of snowmelt in a small area,' *Hydrological Processes*, **13**, 1859-1870. Woo, M-k. & Young, K.L (2000) 'Modelling arctic snow distribution and melt at the 1 km grid scale,' Report for Climate Research Branch, Meteorological Survey of Canada. Unpublished.

Young, K.L. & Lewkowicz, A.G. (1990) 'Surface energy balance of a perennial snowbank, Melville Island, Northwest Territories, Canada,' *Arctic and Alpine Research*, **22** (3), 290-301.